Ecological Modelling 222 (2011) 241–252

Contents lists available at ScienceDirect

Ecological Modelling

journal homepage: www.elsevier.com/locate/ecolmodel

The effects of groundwater table and flood irrigation strategies on soil water and salt dynamics and reed water use in the Yellow River Delta, China

Tao Xie, Xinhui Liu, Tao Sun*

State Key Laboratory of Water Environment Simulation, School of Environment, Beijing Normal University, Beijing 100875, China

ARTICLE INFO

Article history:
Available online 16 March 2010

Keywords:
Groundwater table
Soil water and salinity
Water use
Reed wetland

ABSTRACT

Vegetation management in shallow groundwater table environments requires an understanding of the interactions between the physical and biological factors that determine root-zone soil salinization and moisture. In this study, the effects of groundwater depth and flood irrigation strategies on water and salt dynamics and reed water use were analyzed in the shallow groundwater region of the Yellow River Delta in China using the HYDRUS-1D model. The results indicated that there is a conflict between water, salt stress, and reed water use with variations in groundwater depth. A water table depth of 3.5 m is the minimum limit to maintain a safe level of soil salinity, but at this depth, the environmental stress on reeds is worsened by the decrease in soil water storage. Maintaining the flood pulses on the wetland, especially during May, may be critical for restoring the reed wetland in the Yellow River Delta.

1. Introduction

Plant growth is limited by soil salinity and water scarcity, especially in areas with shallow groundwater. The water flowing upward from the groundwater into the root-zone plays an important role by contributing to the water requirements of plants in the presence of shallow water tables (Ahmad et al., 2002; Yang et al., 2007). Wetlands, especially those depending on rivers, have suffered from ecological degradation and severe reductions in available water during the last century due to intensified agricultural and unsustainable water uses, increased pollution rates, and climatic changes (Zacharias et al., 2005). For instance, in the Yellow River Delta (YRD), China, freshwater wetlands have been degraded due to water deficiencies. Over a long period of time, evapotranspiration without subsurface leaching can result in soil salinization if there is significant salt in the groundwater and soil (Kahlown et al., 2005; Il'Ichev et al., 2008). Salinity can threaten biodiversity and negatively influence soil quality and agricultural production (Chhabra and Kumar, 2008; Geerts et al., 2008; Wang et al., 2008; Gowing et al., 2009). Therefore, it is necessary to assess the salinity hazard, based on the groundwater quality, the plants' salinity threshold, and the overall salt balance, before promoting reliance on water tables for vegetation restoration (Morris and Collopy, 1999; Ahmad et al., 2002; Wang et al., 2004b; Gowing et al., 2009).

Numerous studies have reported on the interactions between the vegetation community, soil characteristics, and water table in the YRD. Xiong et al. (2008) demonstrated that the distribution of different herbaceous vegetation communities in the YRD wetlands was significantly correlated with soil salinity and pH, but not correlated with the total phosphorus, total nitrogen, and organic matter in the soil. Zhang et al. (2007) observed that the soil salt content was an important factor that determined the halarch succession in the YRD. Song et al. (2008) reported that the plant community classifications mainly reflected the variations in soil salt content and groundwater depth, which were determined by the microtopography. Hie et al. (2008) observed that there were niche differentiations of plant species due to water table depth and soil salinity gradients. Cui et al. (2006) and Tan and Zhao (2006) demonstrated that the water table depth significantly influenced reed growth and community distribution. However, very few studies have examined the relations between the groundwater table, flood irrigation, soil water and salt dynamics, and reed water.

In this study, the HYDRUS-1D model was used to simulate soil water and salinity dynamics in reeds based on field observations of soil water, groundwater, and the corresponding salt dynamics in the YRD. HYDRUS-1D (Šimůnek et al., 2005) is a computer model based on the Richards equation for variably saturated water flow and the advection-dispersion equation for solute transport. The model has been successfully applied in numerous studies to analyze site-specific soil salinization, moisture, and plant growth problems (Šimůnek et al., 2008; Forkutsa et al., 2009a,b). The objectives of this paper are to: (1) evaluate the impact of the groundwater table and flood irrigation strategies on reed water use and soil water and salinity dynamics in shallow groundwater table areas of the YRD, and (2) suggest possible water management alternatives to increase reed water use and minimize soil salinity at the field level.

* Corresponding author. Tel.: +86 10 58805053; fax: +86 10 58800830.
E-mail address: suntao@bnu.edu.cn (T. Sun).

0304-3800/$ – see front matter © 2010 Elsevier B.V. All rights reserved.
doi:10.1016/j.ecolmodel.2010.01.012

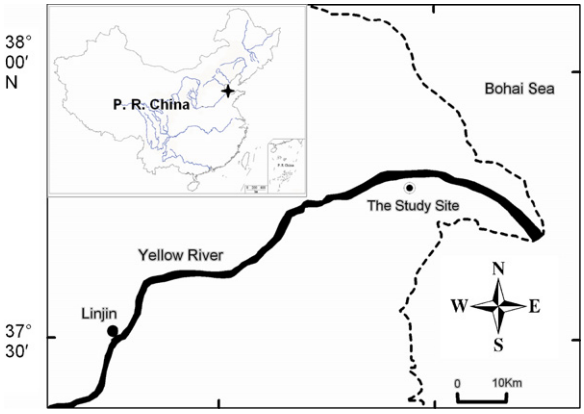

Fig. 1. Geographical location of the study site (Li et al., 1998).

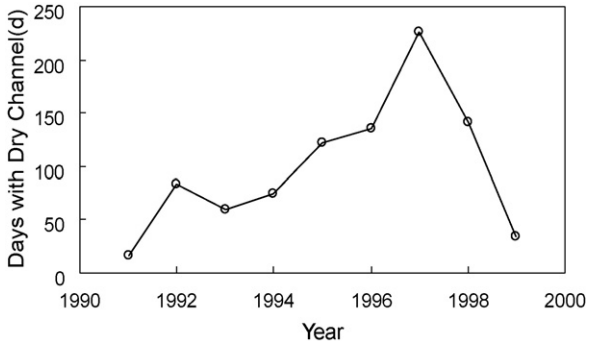

Fig. 2. Number of days the Yellow River Estuary was dry from 1991 to 1999.

2. Materials and methods

2.1. Study area

The Yellow River is the second largest river in China and the sixth largest river in the world in terms of length. The YRD (longitude 117°48′E–119°45′E, latitude: 36°52′N–8°12′N), is situated in the northeast of the Shandong Province, on the southern bank of the Bohai Sea (Fig. 1). The sediment load of the Yellow River is extremely high. Deposition occurs in low-energy areas where the water velocity decreases sufficiently to allow sediment drop out. The YRD is the fastest growing delta in the world and one of the most representative river wetland ecosystems in the world. Under the combined action of freshwater inflow and tide flow, the plants in the YRD exhibit a patchy distribution, and the species composition of the vegetation is very simple. The five dominant species in the YRD are reed (*Phragmites australis* (Cav.) Trin. ex Steud), congongrass (*Imperata cylindrical* var. major), suaeda salsa (*Suaeda heteroptera*), saltcedar (*Tamarix chinensis* Lout.), and willow (*Salix matsudana* Koidz.) (Wang et al., 2004a; Zhang et al., 2007). The YRD has become one of the important habitats for migrating birds in the world and has enormous economic potential for sustainable development because of its geographic position and climatic features. The YRD also performs vast ecological functions, including purifying water resources, decomposing pollutants, supplying groundwater, maintaining regional water balances, and adjusting climatic features.

Since the early 1970s, the Yellow River flow has been decreasing, and the frequency of complete drying or ephemeral flow has been increasing. Additionally, the duration of the dry periods has steadily increased (Liu and Zhang, 2002). In the early 1990s, drying took place annually, with an average of 100 days per year without water in the lower reaches. In 1997, the river was dry for 227 days at Lijin Station, and no water reached the estuary for 330 days (Fig. 2). Meanwhile, the area of native reed wetlands in the YRD significantly decreased, fragmented and degraded (Zong et al., 2008), which greatly threatened rare and endangered species in the region. During this ecological succession, the decline of the reed wetland ecosystems was most greatly impacted by water scarcity and soil salinity and was mainly determined by the groundwater table in the YRD (Tan and Zhao, 2006; Zhang et al., 2007).

Two plots with shallow groundwater tables in the reed wetland of Yellow River Delta National Nature Reserve (37°45′N, 119°01′E) (Fig. 1) were selected for field experiments. The experimental site has a typical monsoon climate with temperatures ranging from 41.9 °C in the summer down to −23.3 °C in the winter. The average annual precipitation is 550–640 mm, with nearly 70% of the precipitation falling between May and September. The mean annual wind speed is 2.98 m s^{-1}, and the frost-free period is 142 days.

Generally, the soil type in the Yellow River Delta National Nature Reserve gradually varies from fluvo-aquic to saline soil, and the soil texture is sand. The soil has a mean bulk density of 1.42 g cm^3 and 1.39 g cm^3 for the 0–150 cm (root-zone) layers in plots I and II, respectively.

The main plant in both plots is reed, which usually bud during the end of March and the first 10 days of April, and head in the middle 10 days of October.

The two observation plots are located approximately 200 m apart. Plot I is in the vicinity of (about 10 m to) an irrigation channel of the Yellow River, and the shallow groundwater of this site is recharged by the fresh water from the channel. So the average annual groundwater salinity of plot I (10 dS m^{-1}) is significantly lower than that of plot II (15 dS m^{-1}). Moreover, since the terrain of plot I is higher than that of plot II, the average annual groundwater depth of plot I (2.0 m) is deeper than that of plot II (1.5 m).

2.2. The HYDRUS-1D model

The HYDRUS-1D model was used in this study in order to identify the effects of water–salt stress on the water use of the typical reed plant in the YRD and the influence of ground water.

2.2.1. Water transport

The Richards' equation was used to describe the soil water flow:

$$\frac{\partial\theta}{\partial t} = \frac{\partial\theta}{\partial z}\left[K\left(\frac{\partial\theta}{\partial h}+1\right)\right] - S(z,t) \quad (1)$$

where θ is the volumetric water content [L^3 L^{-3}], K is the unsaturated hydraulic conductivity function [T^{-1}], t is time [T], h is the water pressure head [L], z is the spatial coordinate [L] (positive upward), and S is the sink or source term for water [L^3 L^{-3} T^{-1}], which represents the water uptake by the plant roots. S was described by the following equation:

$$S = \alpha(h, h_\Phi)b(z)T_p \quad (2)$$

where $\alpha(h, h_\Phi)$ is the root water uptake reduction function, h_Φ is the soil water osmotic head [L], $b[z]$ is the normalized water uptake distribution [L^{-1}], and T_p [L^3 L^{-2} T^{-1}] is the potential transpiration.

The multiplicative S-shaped model introduced by van Genuchten (1987) was used to describe the uptake reduction function:

$$\alpha(h, h_\Phi) = \frac{1}{1+(h/h_{50})^{p_1}} \cdot \frac{1}{1+(h_\Phi/h_{\Phi 50})^{p_2}} \quad (3)$$

where p_1 and p_2 are experimental constants. The parameter h_{50}[L] and $h_{\Phi 50}$[L] represent the pressure head and osmotic head at which

the water uptake rate are reduced by 50% during conditions of negligible water and osmotic stress, respectively.

The soil water retention ($\theta(h)$) and hydraulic conductivity ($K(h)$) variables in Eq. (1) were described using van Genuchten's (1980) functions as follows:

$$\theta = \begin{cases} \theta_r + \dfrac{\theta_s - \theta_r}{(1 + |ah|^n)^m} & h < 0 \\ \theta_s & h \geq 0 \end{cases} \quad (4)$$

$$K(h) = K_s S_e^l [1 - (1 - S_e^{1/m})^m]^2 \quad (5)$$

where θ_r and θ_s are the residual and saturated water contents [$L^3\,L^{-3}$], respectively, which can be determined by the field data. K_s [$L\,T^{-1}$] is the saturated hydraulic conductivity, α [L^{-1}] and n represent the empirical shape parameters, $m = 1 - 1/n$, and l is a pore connectivity parameter. To reduce the number of free parameters, we took $l = 0.5$, a common assumption which was based on the work of Mualem (1976). S_e is the effective saturation, given by:

$$S_e = \frac{\theta - \theta_r}{\theta_s - \theta_r} \quad (6)$$

2.2.2. Solute transport

The partial differential equation governing one-dimensional, convective-dispersive mass transport under transient water flow conditions in a partially saturated porous medium is represented by the following equation:

$$\frac{\partial \theta c}{\partial t} = \frac{\partial \theta}{\partial z}(\theta D \frac{\partial c}{\partial z}) - \frac{\partial qc}{\partial z} \quad (7)$$

where c is the solute (salt) concentration [$M\,L^{-3}$]. D is the effective dispersion coefficient [$L^2\,T^{-1}$], and q is the volumetric flux density given by Darcy's law [$L^3\,L^{-2}\,T^{-1}$]. D is described by the following equation:

$$D = a_L q \quad (8)$$

where α_L represents the longitudinal dispersivity [L]. Eq. (8) assumes that molecular diffusion is insignificant relative to dispersion.

2.2.3. Boundary condition

Groundwater depth measurements were used to describe the bottom boundary of the soil profile. There was no noticeable surface runoff during the study period, and the top boundary conditions were defined by evaporation and precipitation. Potential evapotranspiration (ET_p) was estimated by the Penman–Monteith equation, using daily weather measurements, such as solar radiation, air temperature, humidity, and wind speed, as well as crop characteristics, such as minimum crop resistance, surface albedo, and crop height (Allen et al., 1998). Potential evaporation (E_p) and potential transpiration (T_p) (root water uptake) were calculated according to the FAO-56 approach and adjusted using the observed leaf area index (LAI) data (Allen et al., 1998) as follows:

$$E_p(t) = ET_p(t) \cdot \exp^{-\beta \cdot \mathrm{LAI}(t)} \quad (9)$$

$$T_p(t) = ET_p(t) - E_p(t) \quad (10)$$

where β (=0.39) is the radiation extinction coefficient.

For salt transport, we implemented a no flux boundary condition at the soil surface. In case of rainfall, this condition assumes that the rain water is free of solute. The measured groundwater electrical conductance (EC_{gw}, $dS\,m^{-1}$) was used to define the lower solute transport boundary.

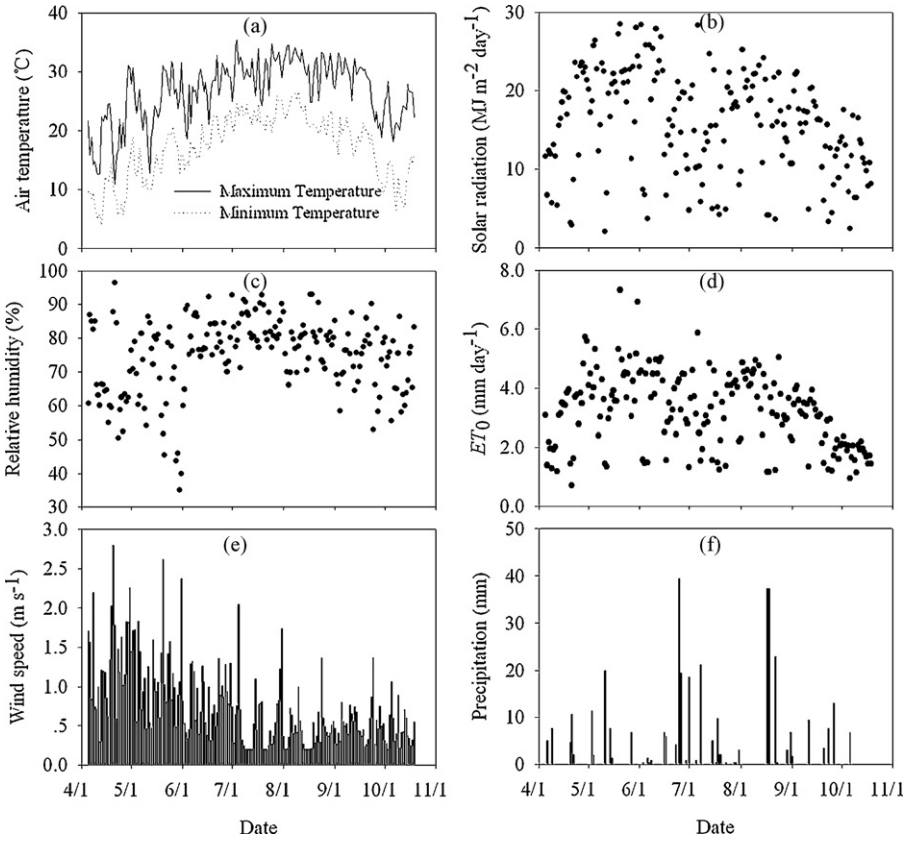

Fig. 3. (a) Air temperature, (b) solar radiation, (c) relative humidity, (d) reference evapotranspiration (ET_0), (e) wind speed, and (f) precipitation measurements from April 5 to October 18, 2008 in the study area.

Table 1
Calibrated soil water conductive parameters.

Plot no.	Depth (cm)	θ_r (cm^3 cm^{-3})	θ_s (cm^3 cm^{-3})	α (cm^{-1})	n	K_s (cm d^{-1})	l
I	0–70	0.01	0.42	0.014	1.04	403	0.5
	70–125	0.03	0.41	0.017	1.08	466	0.5
	125–350	0.04	0.45	0.019	1.05	399	0.5
II	0–40	0.02	0.41	0.015	1.10	650	0.5
	40–125	0.07	0.41	0.008	1.11	236	0.5
	125–350	0.02	0.46	0.022	1.10	425	0.5

Note: parameters α, n and K_s were optimized.

2.3. Data collection

In this study, various input parameters needed for calibration and validation of the HYDRUS-1D model were collected in plots I and II from April 5 (the start of reed germination) to October 18 (when the reeds finished heading) in 2008.

2.3.1. Climatic data

Daily meteorological data, including the maximum and minimum temperature, rainfall, humidity, solar radiation, and wind velocity (Fig. 3), were obtained from a weather station 2 km away from the study site.

2.3.2. Soil water content and salinity in the root-zone

Each plot was equipped with one neutron probe access tube to measure the soil water content, and measurements were made every 10 cm down to a depth of 150 cm. Seven calibrated TYC-2 salt sensors (Institute of Soil Science, Chinese Academy of Sciences, China) were installed vertically at depths of 10, 20, 30, 50, 70, 100 and 120 cm in each plot to measure the soil solution electrical conductivity (EC, dS m^{-1}). In this study, the soil water osmotic heads h_Φ and salt concentration in the soil water (c) were assumed to be a linear function of EC, according to the following equation (Richards, 1954; Homaee et al., 2002a; Zuo et al., 2004):

$$h_\Phi = -36c = 360EC \quad (11)$$

where h_Φ is expressed in cm, and c (expressed as the cation concentration) has units of milliequivalents per liter of water (meq L^{-1}).

2.3.3. Ground water dynamics

Two shallow monitoring wells were installed in the vicinity of the two plots, respectively. One Odyssey Capacitance Water Level Recording System (Dataflow Systems Pty Ltd., Odyssey House, New Zealand) was installed in each well to measure the groundwater level. The groundwater electrical conductivity EC_{gw} was measured once every 5 days.

2.3.4. Plant growth and root uptake function

The leaf area index (LAI) was measured biweekly, and the reed height (H) was measured weekly at each plot (Fig. 4). Root lengths (L_r, cm) were measured in a randomly selected 1 m^2 quadrant in the study plot once every three months. Root lengths of the rhizome-grown reed did not significant increase during the simulating period. Therefore, the rooting depth was assumed to be fixed at 1.5 m for this study. The root length density distribution was assumed to decline linearly with depth.

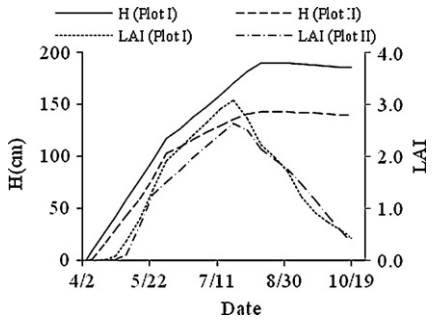

Fig. 4. The leaf area index (LAI) and height (H) of the reeds in plots I and II.

For the HYDRUS-1D model used in our study, the computer analyses simulated root water uptake as a function of water and salinity stress. Less attention was paid to the reed root water uptake, and it was not possible to reliably describe the water uptake function for reeds. In this study, a reed culture experiment in the YRD was performed using the method of Homaee et al. (2002b) to determine the root uptake reduction function (Eq. (3)). The experimental data was best fit in Eq. (3) when $h_{50} = -2456$ cm, $p_1 = 3$, $h_{\Phi 50} = -6500$ cm, and $p_2 = 2.3$ ($R^2 = 0.89$). These parameters were subsequently incorporated into the HYDRUS-1D model.

2.4. Calibration and validation of HYDRUS-1D model

The HYDRUS-1D model was calibrated based on the volumetric water content, θ, and the soil water electrical conductivity, EC, measured from the soil profiles in the two observation plots. The calibration period was from April 5 to July 22, 2008, and the verification period was from August 3 to October 18, 2008.

The soil hydraulic properties, residual and saturated water contents (θ_r and θ_s), were measured in the laboratory from soil samples that were extracted from the observation plots. The saturated hydraulic conductivity (K_s) was evaluated at the fields. K_s and the empirical shape parameters, α and n, were optimized using the Levenberg–Marquardt method that was incorporated in the HYDRUS-1D code (Šimůnek et al., 2005). During the inverse calibration process, the K_s range was settled as 200–700 cm d^{-1} based on measurements made in the study area, and θ_s and θ_r were fixed according to the measured values in the laboratory. The α_L parameter was set at 12 cm by using trial and error, and we assumed that α_L was invariant with time and depth at the field site (Abbasi et al., 2003; Crescimanno and Garofalo, 2005). Each inverse problem was restarted several times using different initial estimates of the optimized parameters. The run with the lowest objective function value was assumed to represent the global minimum. The calibrated soil hydraulic parameters are shown in Table 1. As the soil texture in both plots was sand, similar soil hydraulic properties with relative high hydraulic conductivity were obtained in both plots.

The root mean square error ($RMSE$) was used to compare the modeling performances and was calculated using the following

Table 2
The $RMSE$ and N of θ and EC for the calibration and validation periods.

Plot no.	θ (cm^3 cm^{-3})				EC (dS m^{-1})			
	Calibration		Validation		Calibration		Validation	
	N	$RMSE$	N	$RMSE$	N	$RMSE$	N	$RMSE$
I	60	0.010	54	0.014	77	1.57	77	2.66
II	60	0.014	54	0.019	77	1.37	77	2.50

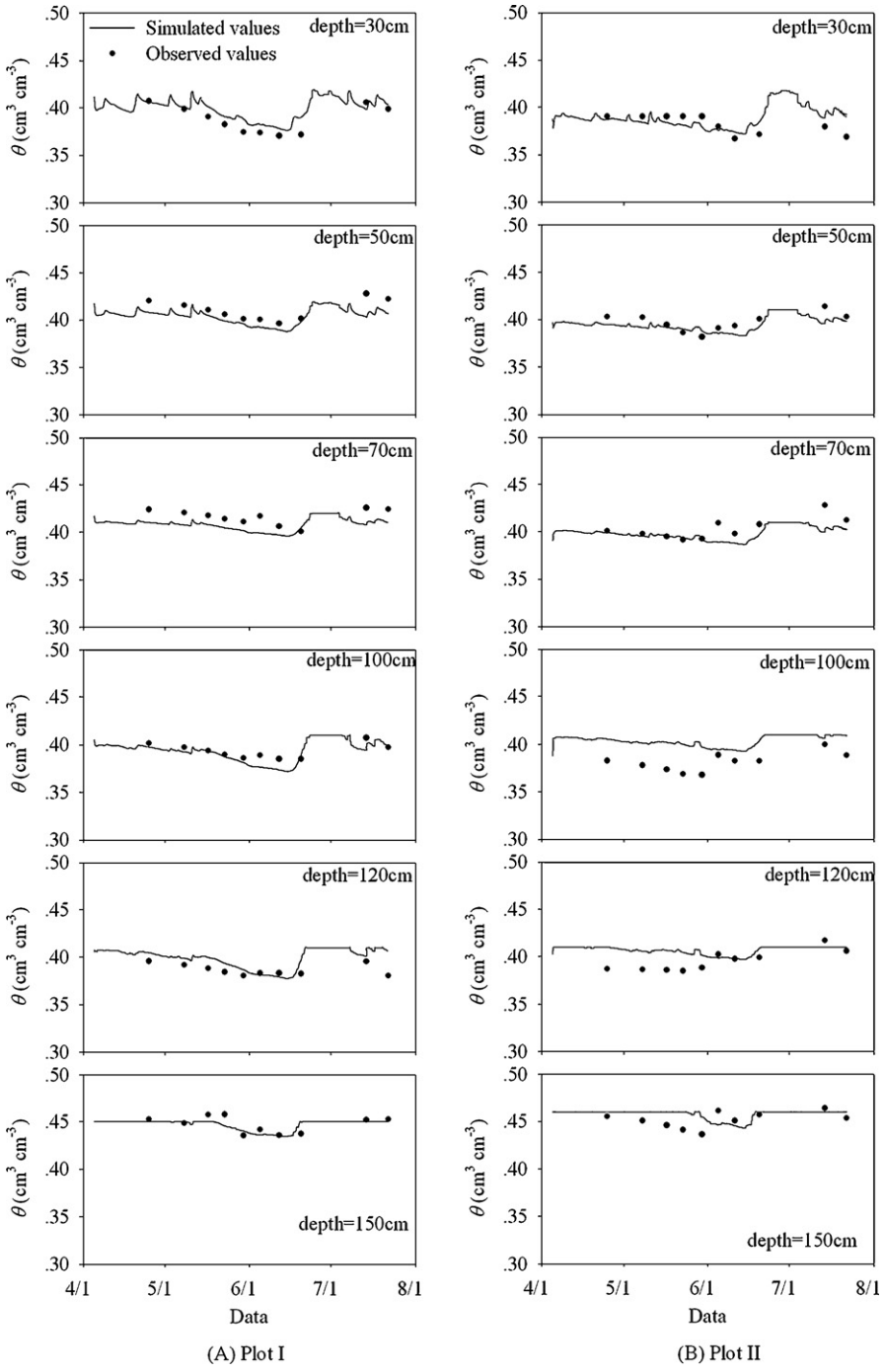

Fig. 5. Measured and fitted soil water content (θ) at different soil depths in plots I and II during the calibration period.

equation:

$$RMSE = \left[\frac{\sum_1^N (O_i - P_i)^2}{N}\right]^{0.5} \quad (12)$$

where P_i and O_i are the predicted and observed values, respectively, and N is the number of observations.

The *RMSE* of θ and *EC* for both the calibration and validation periods is shown in Table 2. During the calibration period, the *RMSE* of θ and *EC* ranged from 0.010 to 0.014 $cm^3\,cm^{-3}$ and 1.37 to 1.57 $dS\,m^{-1}$, respectively. During the validation period, the *RMSE* of θ and *EC* ranged from 0.014 to 0.019 $cm^3\,cm^{-3}$ and 2.50 to 2.66 $dS\,m^{-1}$, respectively. The model correctly predicted the observed soil water content, but was less accurate in predicting the salt concentration of the soil solution, probably because of locally occurring chemical processes, such as adsorption–desorption and proportional root uptake (Šimůnek et al., 2005), not accounted for by the model.

Both the simulation results for θ (Figs. 5 and 6) and *EC* (Figs. 7 and 8) showed the same tendencies as the measured values. The differences between the observed and simulated θ and *EC* values were partly due to spatial heterogeneity and observation errors, which are inevitable under field conditions (Singh et al., 2006; Vazifedoust et al., 2008).

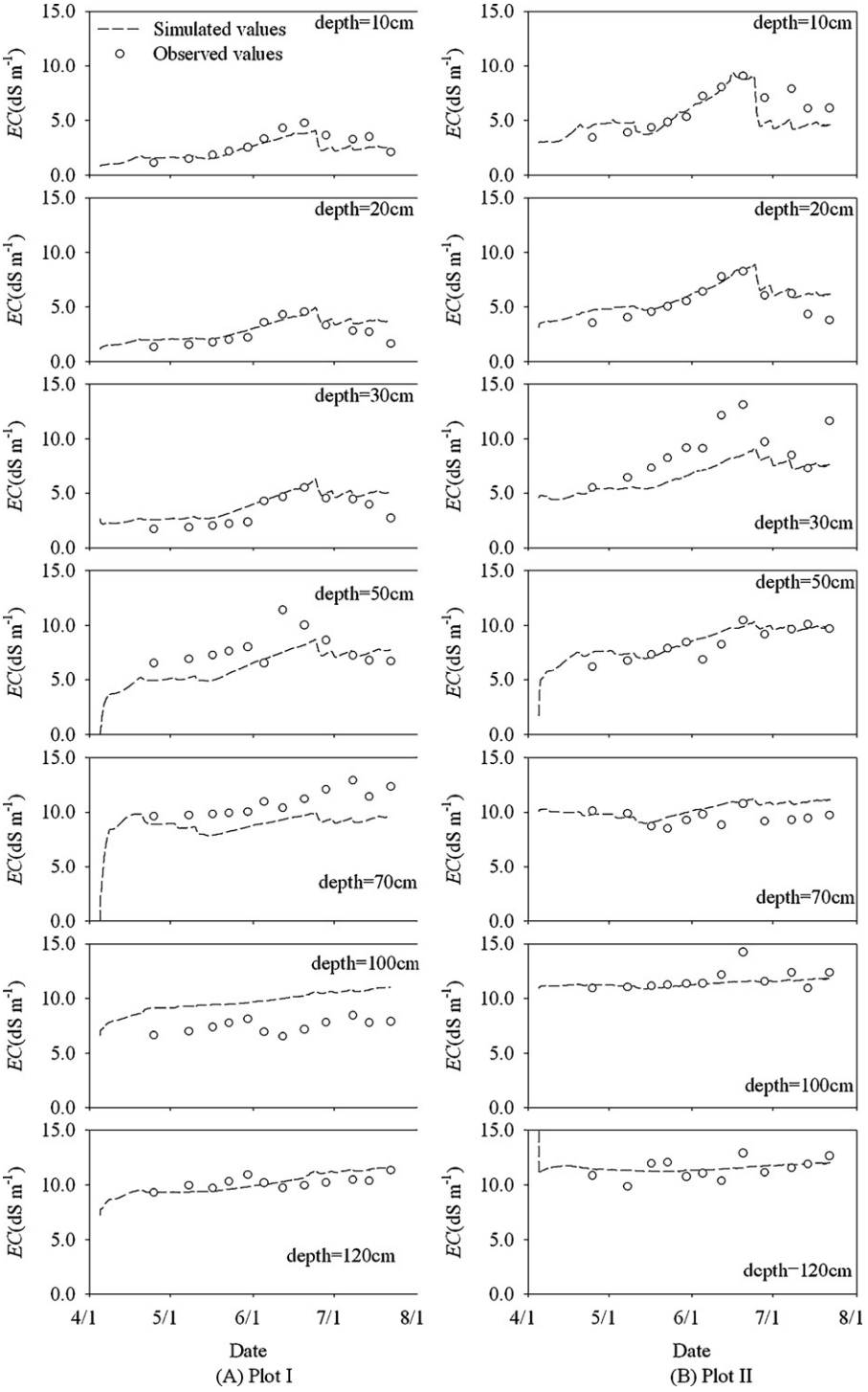

Fig. 6. Measured and simulated soil water content (θ) at different soil depths in plots I and II during the validation period.

2.5. Management strategies analysis

After validating the HYDRUS-1D model, two types of different water management strategies were simulated. The aim was to identify a groundwater depth that was sufficient to control the soil salinity at safe level and also meet the reed water requirements in the YRD. To accomplish this aim, we analyzed the effects of the groundwater table control on the soil water and salt balance, and on reed water use without irrigation events in the YRD. We considered several groundwater depths from 0.5 m to 3.5 m.

To describe the influence of different flood irrigation periods and amounts on reed water use, we simulated two possible flood irrigation periods and three irrigation amounts (1 cm d^{-1}, 3 cm d^{-1} and 5 cm d^{-1}). In order to promote soil desalinization at the beginning of the reed's fast growing period, we set one irrigation period from May 15th to May 29th. The other irrigation period was set from June 23rd to July 7th, which was during the Yellow River's water and sediment regulation period. It is easy to divert flood water for irrigation during that time. In both of these irrigation strategies, the irrigated water was added to the water from precipitation, and we used the atmospheric boundary condition with

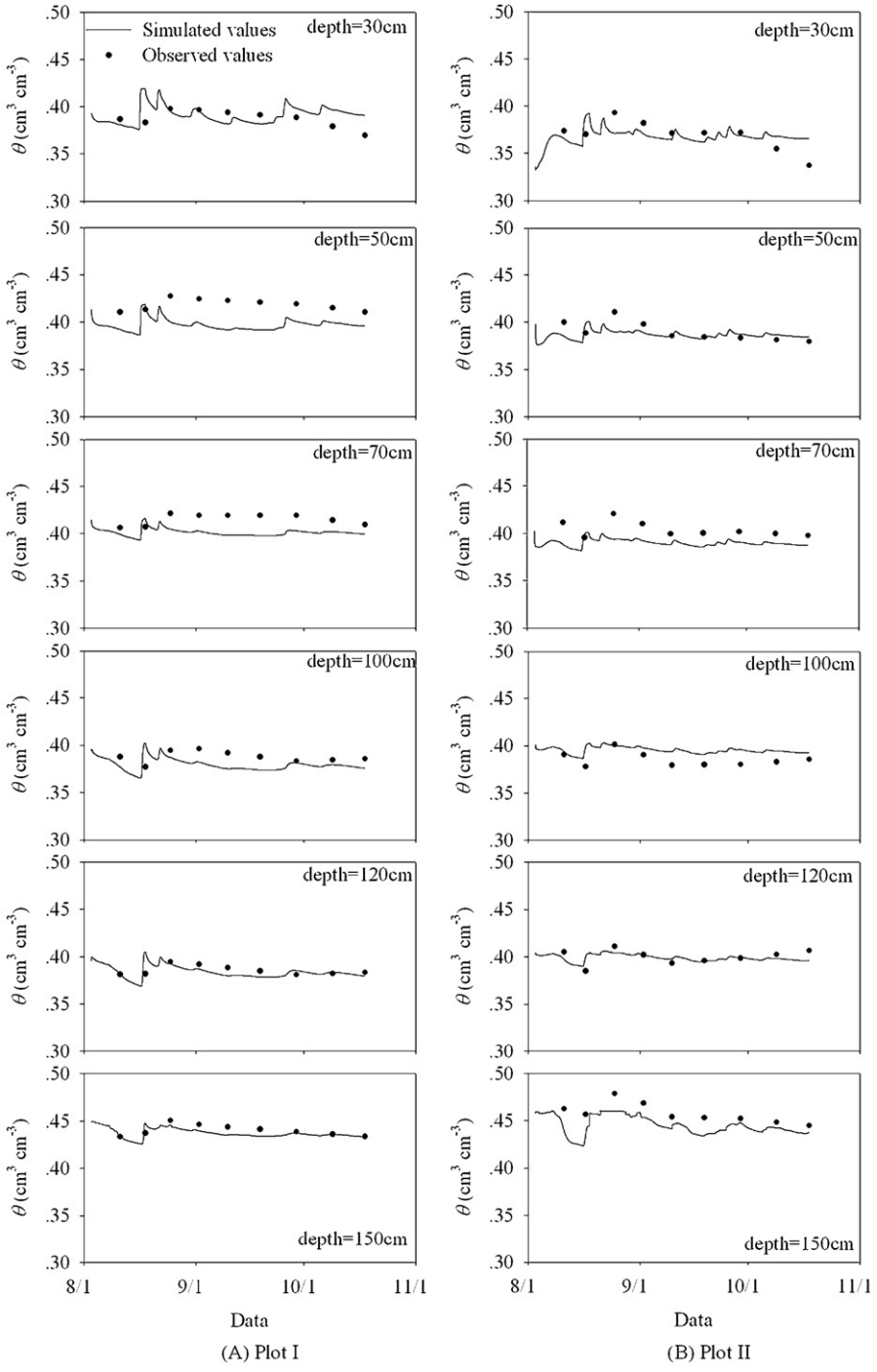

Fig. 7. Measured and fitted soil solution electrical conductivity (*EC*) at different soil depths in plots I and II during the calibration period.

surface run off (Šimůnek et al., 2005). During the simulation, the irrigated water electrical conductance was set at 1.1 dS m^{-1}, which corresponded to the electrical conductance of the freshwater in the channel connected to the Yellow River.

In all of these scenarios, the plant, initial soil water, and soil water salinity data matched those observed in plot I. The simulation period was from April 5th to October 10th and was based on the meteorological data collected in 2008.

3. Uncertainty and sensitivity assessment

There are two types of potential sources of uncertainty for the computed cumulative actual transpiration (Cum. T_a/cm) in our modeling approach. On one hand, sources of uncertainty include the values of various model parameters such as the parameters of root uptake function in Eqs. (3) and the soil hydraulic parameters in Eqs. (4) and (5). On the other hand, source of uncertainty involves extrapolation of the field results to the larger region. However, an accurate characterization of prediction uncertainty is problematic because of a lack of knowledge about the underlying parameter variability and parameter correlation structure at multiple levels (Jiménez-Martínez et al., 2009).

In this study, the importance of parameter uncertainty was estimated by performing a sensitivity analysis. For this analysis, the effect of ±10% parameter perturbations on the calculated Cum. T_a was evaluated. Parameters considered for sensitivity analyses

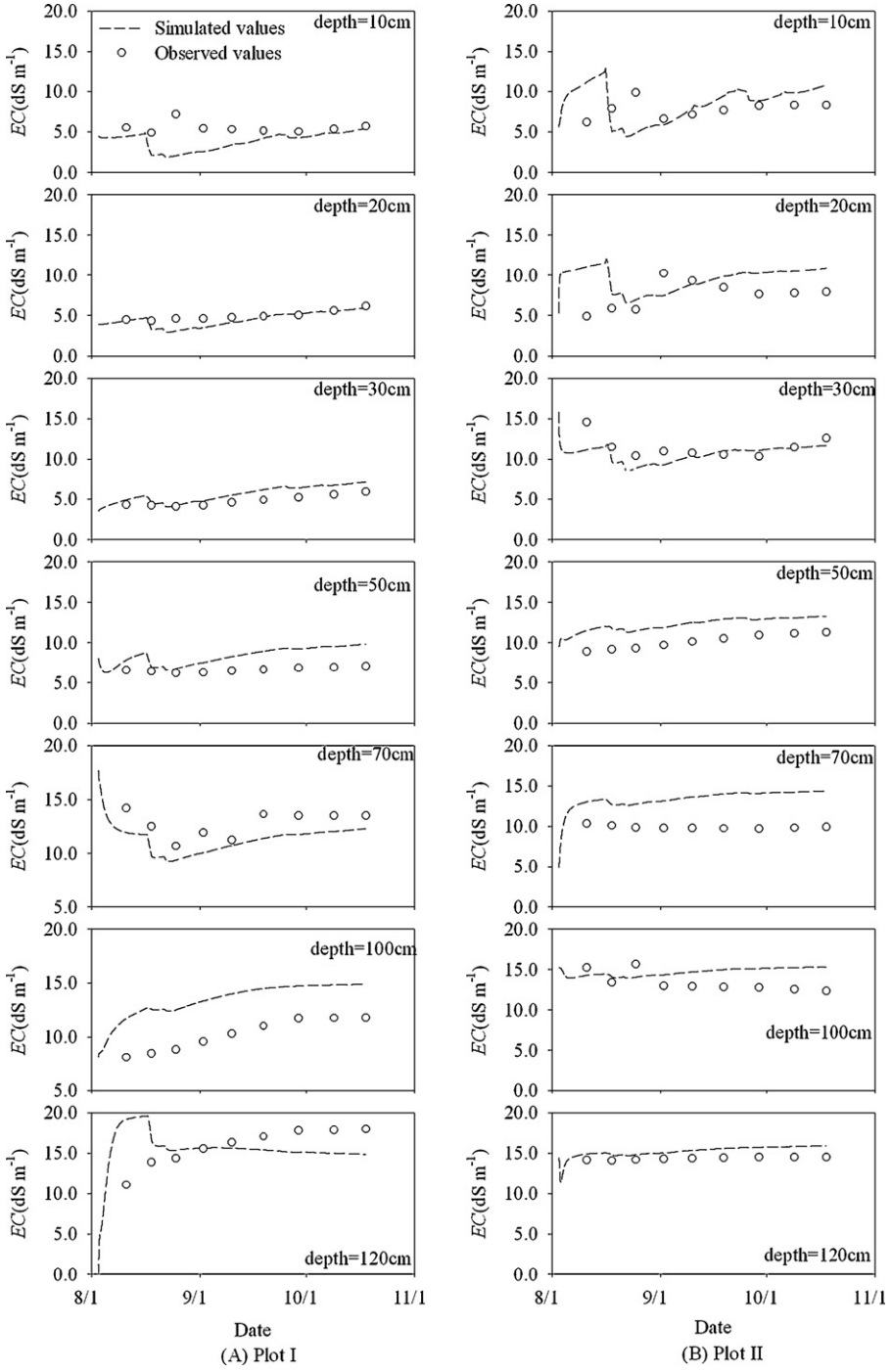

Fig. 8. Measured and simulated soil solution electrical conductivity (*EC*) at different soil depths in plots I and II during the validation period.

were θ_s, θ_r, a, n, K_s, l, p_1, p_2, h_{50} and $h_{\Phi 50}$. While the simulation for a −10% perturbation of n was not completed, because the small n value caused numerical difficulties in the simulation model (a well-known problem for $n \rightarrow 1$).

The sensitivity analysis results for the soil hydraulic parameters showed that computed Cum. T_a was least sensitive to θ_r, a, K_s and l. ±10% perturbation of these parameters in any of the three soil layers resulted in a change to the computed Cum. T_a of less than 2%. Relatively high sensitivity in the surface soil layer was found for θ_s and n, respectively. ±10% perturbation of θ_s altered Cum. T_a that ranged from 6% to 60% in the surface soil layer and 1–15% in the bottom two layers. 10% perturbation of n altered Cum. T_a by 6% in the surface soil layer and between 1% and 3% in the bottom two layers.

The final sensitivity calculations involved ±10% perturbations to the parameters of root uptake function (p_1, p_2, h_{50} and $h_{\Phi 50}$). The computed Cum. T_a was relatively insensitive to the perturbations of p_1 and h_{50}, with the computed Cum. T_a changing by less than 1%. Greater sensitivity was found for p_2 and $h_{\Phi 50}$, where the ±10% perturbations altered the computed Cum. T_a by about 1–3%. This implies that reed water use is more sensitive to salt stress than water stress in the study site.

However, as it is impossible to confirm the sources of uncertainty with sensitivity analysis, future work aimed at quantifying

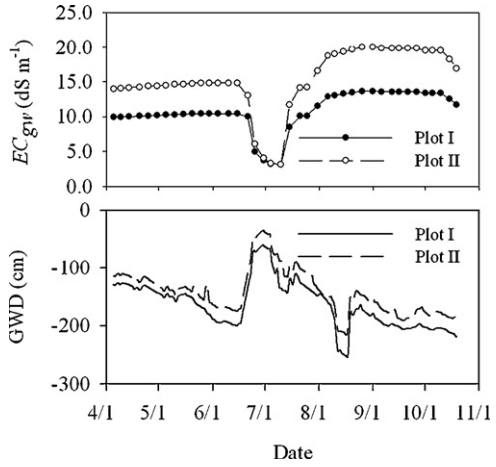

Fig. 9. Groundwater depths (GWD) and electrical conductivity (EC_{gw}) measurements from April 5 to October 18, 2008 in plots I and II.

uncertainty in all parameters above would greatly benefit efforts to determine uncertainty in Cum. T_a calculations.

4. Results and discussions

4.1. Groundwater dynamics

Fig. 9 shows the temporal variations in groundwater depth and EC_{gw}. Similar trends were observed in the changes in groundwater depth and electrical conductivity in both plots. During the study period, the groundwater ranged from 0.7 m to 2.5 m in plot I and from 0.4 m to 2.1 m in plot II, respectively. The groundwater salinity ranged from 3 dS m^{-1} to 14 dS m^{-1} in plot I and from 3 dS m^{-1} to 20 dS m^{-1} in plot II. A sharply increasing trend in groundwater depth and a decreasing trend in salinity were observed from June 23 to July 8, 2008. These trends resulted from water and sediment regulation of the Yellow River during that period.

4.2. Soil water and salt dynamics and reed water use

The high soil moisture content during the entire reed-growing season is clearly shown in Figs. 5 and 7. We did not observe clear water stages in the root-zone that included alternations between dry and wet periods in the two plots. This was mainly because of the frequent rainfall and the shallow groundwater table during the study period. The simulations of cumulative water fluxes for both plots are shown in Fig. 10. The total infiltration during the study period was 37 cm in both plots, which was much lower than the

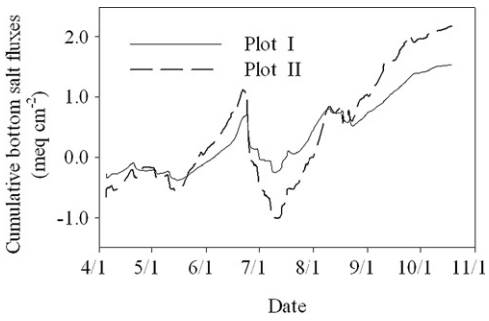

Fig. 11. Cumulative bottom salt fluxes in plots I and II from April 5 to October 18, 2008.

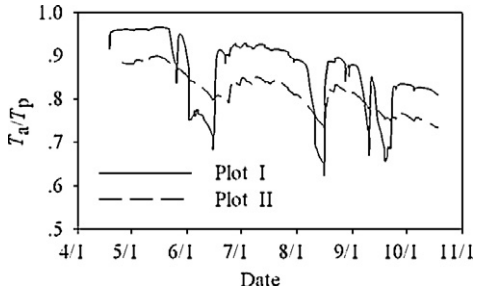

Fig. 12. Relative transpiration (T_a/T_p) of reeds from April 5 to October 18, 2008.

cumulative evapotranspiration, which is the sum of the cumulative actual transpiration (T_a) and evaporation (E_a). The total cumulative bottom water fluxes in both plots showed increasing trends during the study period, which indicated that there was a direct groundwater contribution to evapotranspiration at the study site.

It was assumed that the soil salinity came entirely from the groundwater and was leached by the drainage water. The bottom salt fluxes (Fig. 11) in both plots showed increasing trends indicating that soil salinization occurred during the study period, which was harmful to reed water use and growth.

Reed water use (transpiration) in the study site increased sharply in mid-May and began to slow down after August because of the decrease of LAI. The reed water use in plot I (29.7 cm) was higher than that in plot II (25.0 cm), which may be explained by the better growth conditions of the reeds in plot I. The simulations indicated that the transpiration of reeds in both plots was likely hampered by salt stress. The relative transpiration rate (T_a/T_p) dropped to approximately 0.7 or below during periods of low rainfall (Fig. 12). Frequent rainfall could not keep the T_a/T_p at a high level during the entire reed growth season.

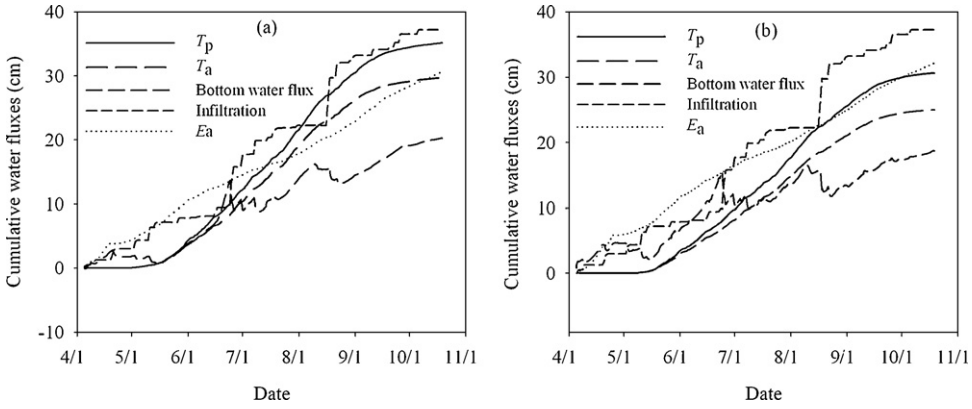

Fig. 10. Cumulative water fluxes (T_p, potential transpiration; T_a, actual transpiration; E_a, actual evaporation) in (a) plot I and (b) plot II from April 5 to October 18, 2008.

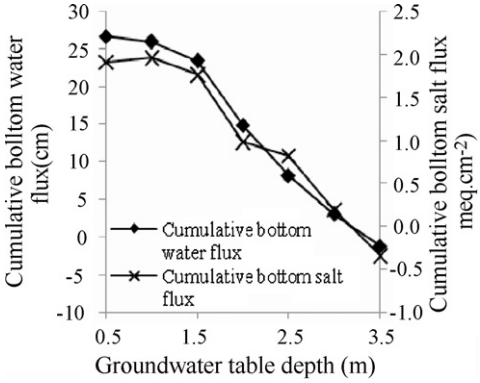

Fig. 13. Cumulative bottom flux and cumulative bottom salt flux at different groundwater depths (GWD).

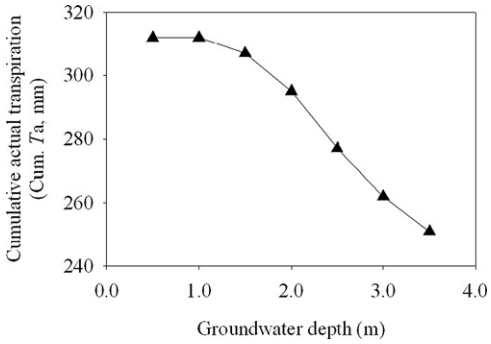

Fig. 14. Cumulative actual transpiration (Cum. T_a) at different groundwater depths.

4.3. Management strategy analyses

4.3.1. Effects of groundwater table on reed water use

Both the cumulative bottom water flux and salt flux decreased with the decline of the groundwater table, and their values were both negative at a groundwater depth of 3.5 m (Fig. 13). These results indicate that below this depth, soil desalinization occurred with the groundwater recharge. However, the environmental stress on the reeds was not effectively alleviated with the decline of salt storage because of a concurrent decrease in soil water storage. The simulated cumulative potential transpiration of the reeds (35.1 cm) was much higher than the reed water use in all scenarios (Fig. 14). The relative transpiration (T_a/T_p) in the reeds significantly decreased with the decline of the groundwater table, especially when the groundwater depth was greater than 1.0 m (Fig. 15). This implies that desalination of saline soils in the study area by controlling the groundwater table below 3.5 m will negatively influence reed water use. It appears difficult to identify a groundwater depth that sufficiently controls soil salinity at safe level and at the same time meets the reed water requirements in the YRD. Frequent flood irrigation of the area with freshwater from Yellow River is necessary for reed recovery.

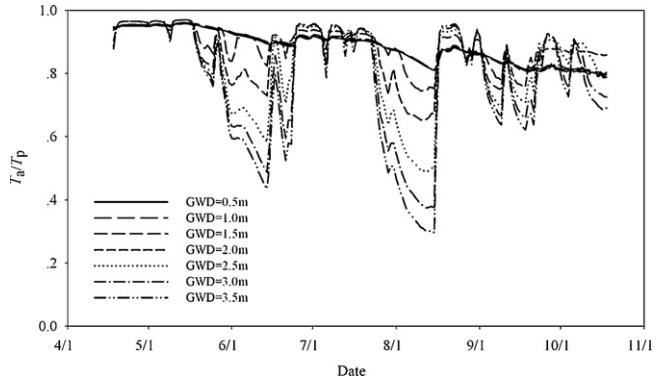

Fig. 15. Relative transpiration (T_a/T_p) of reeds at different groundwater depths (GWD).

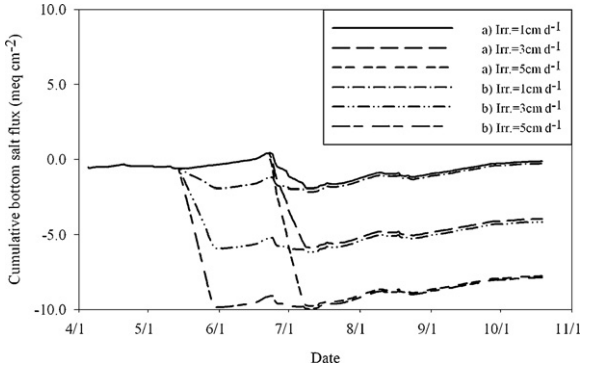

Fig. 16. Cumulative bottom salt fluxes under different irrigation strategies (Irr., irrigation water amounts). (a) Irrigation during the Yellow River water and sediment regulation period (June 23–July 7). (b) Irrigation during the reed's fast growing period (May 15–May 29).

4.3.2. Effects of different flood irrigation strategies on reed water use

Two ecological water supplement strategies were simulated to analyze the influence of different flood irrigation periods and amounts upon reed water use. The earlier irrigation strategy was conducted from May 15 to May 29 at the beginning of the reed's fast growing period, while the latter irrigation strategy was carried out from June 23 to July 7 during the Yellow River's water and sediment regulation period. For each simulation, the irrigation period was 15 days. The cumulative bottom salt fluxes were negative in both irrigation strategies (Fig. 16), indicating that the soil salt accumulation could be efficiently controlled. Additionally, this indicated that there were no significant differences between the cumulative bottom salt fluxes of the two strategies at the end of the study period.

The cumulative actual transpiration (Cum. T_a/cm) under the different irrigation strategies are shown in Table 3. For both irrigation strategies, irrigation increased the reed water use when compared to the cumulative actual transpiration (29.7 cm). The reed water use was improved with the increase of irrigation water amounts. Additionally, the earlier irrigation strategy improved the reed water more than the latter irrigation strategy. These differences were for a number of reasons: (1) during the period from May 15 to May 29, precipitation was relative lower than during the period from June 23 to July 7, (2) the groundwater table sharply increased during the Yellow River's water and sediment regulation period (Fig. 9), which decreased the efficiency of irrigated water use, (3) the relative transpiration (T_a/T_p) (Fig. 17) under different irrigation strategies indicated that the water stress on reeds that occurred before mid-June was not alleviated by the latter irrigation strategy. Moreover, in the earlier irrigation strategy, 15 days of flood

Table 3
Cumulative actual transpiration (Cum. T_a/cm) under different irrigation strategies.

Irrigation period	Irrigation water amounts (Irr.)		
	1 cm d^{-1}	3 cm d^{-1}	5 cm d^{-1}
May 15–May 29	32.0	34.0	34.4
June 23–July 7	31.1	32.7	33.0

Note: the cumulative potential transpiration was 35.1 cm.

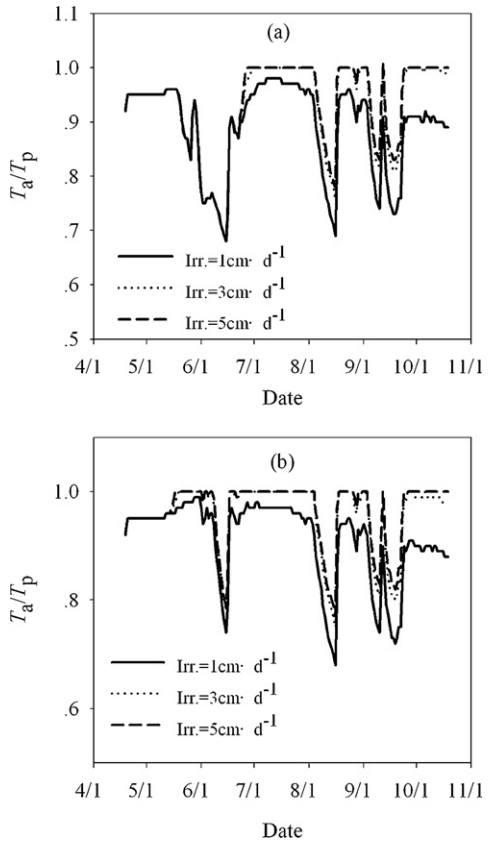

Fig. 17. Relative transpiration (T_a/T_p) of reeds under different irrigation strategies (Irr., irrigation water amounts). (a) Irrigation during the Yellow River's water and sediment regulation period (June 23–July 7). (b) Irrigation during the reed's fast growing period (May 15–May 29).

irrigation at 3 cm d^{-1} produced a cumulative actual transpiration (34.0 cm) that was close to the cumulative potential transpiration (35.1 cm). Therefore, the earlier irrigation strategy would more successfully increase reed water use and be helpful for reed recovery in the YRD.

5. Conclusions

Vegetation management in shallow groundwater table environments requires an understanding of the interactions between the physical and biological factors that determine the root-zone soil salinization and moisture. The field soil water and salt dynamics were observed during the reed-growing season from April 5 to October 18. The maintenance of higher soil water content and soil salt accumulation was observed during the reed-growing season in shallow groundwater environments in the YRD. The actual transpiration of the reeds was often lower than the potential rate mainly because of the salinity stress in this region.

This study compared HYDRUS-1D simulations of soil water and salt dynamics with field observation data collected from the study site in the YRD. Acceptable agreement between the model simulations and the observed data was achieved. This implies that the HYDRUS-1D model can be a useful tool for water management in this region.

Several scenarios have been generated to better understand the effect of the groundwater table on the water and salt balance and reed water use in the YRD. The results indicated that there is a conflict between the water, salt stress and reed water use that is related to variations in the groundwater depth. A water table depth of 3.5 m is the minimum limit to maintain a safe level of soil salinity, but at this depth, the environmental stress on reeds is worsened by the decrease in soil water storage. The water requirements and a safe level of salinity could not be established by varying the groundwater depth.

Two ecological water supplement strategies were simulated to analyze the influence of different flood irrigation periods and amounts on reed water use. The results demonstrate that irrigation can clearly increase the reed water, especially when the irrigated water amounts are higher than 3 cm d^{-1}. However, the water stress on the reeds could not be better alleviated by using the irrigation strategy from June 23 to July 7 during the Yellow River's water and sediment regulation period than using the irrigation strategy from May 15 to May 29 during the fast growing period of reed. This implies that earlier irrigation efforts in May would be more helpful to increase reed water use and aid reed recovery in the YRD. Maintaining the flood pulses on the wetland, especially during the month of May, may become critical to restore the reed wetland in the YRD.

The groundwater table in the YRD is sharply affected by the fresh water discharge quantity in the lower Yellow River. In the future, a larger scale and longer term study that simulates the interactions between the lower Yellow River water discharge, groundwater regime, and vadose zone would be useful to understand the influence of the lower Yellow River water regime on the reed meadow wetland in the YRD.

Acknowledgements

This work was supported by the National Science Foundation for Distinguished Young Scholars (50625926) and the National Basic Research Program of China (973) (Grant 2006CB403303).

References

Abbasi, F., Simunek, J., Feyen, J., van Genuchten, M.T., Shouse, P.J., 2003. Simultaneous inverse estimation of soil hydraulic and solute transport parameters from transient field experiments: homogeneous soil. Trans. ASAE 46, 1085–1095.

Ahmad, M.U.D., Bastiaanssen, W.G.M., Feddes, R.A., 2002. Sustainable use of groundwater for irrigation: a numerical analysis of the subsoil water fluxes. Irrig. Drain. 51, 227–241.

Allen, R.G., Pereira, L.S., Raes, D., Smith, M., 1998. Crop Evapotranspiration – Guidelines for Computing Crop Water Requirements – FAO Irrigation and Drainage Paper 56. Food and Agriculture Organization of the United Nations, Rome.

Chhabra, R., Kumar, A., 2008. Effect of water-table depths and groundwater salinities on the growth and biomass production of different forest species. Indian J. Agric. Sci. 78, 785–790.

Crescimanno, G., Garofalo, P., 2005. Application and evaluation of the SWAP model for simulating water and solute transport in a cracking clay soil. Soil Sci. Soc. Am. J. 69, 1943–1954.

Cui, B.S., Zhao, X.S., Yang, Z.F., 2006. The response of reed community to the environment gradient of water depth in the Yellow River Delta. Acta Ecol. Sin. 26, 1154–1533 (in Chinese).

Forkutsa, I., Sommer, R., Shirokova, Y.I., Lamers, J.P.A., Kienzler, K., Tischbein, B., Martius, C., Vlek, P.L.G., 2009a. Modeling irrigated cotton with shallow groundwater in the Aral Sea Basin of Uzbekistan: I. Water dynamics. Irrig. Sci. 27, 331–346.

Forkutsa, I., Sommer, R., Shirokova, Y.I., Lamers, J.P.A., Kienzler, K., Tischbein, B., Martius, C., Vlek, P.L.G., 2009b. Modeling irrigated cotton with shallow groundwater in the Aral Sea Basin of Uzbekistan: II. Soil salinity dynamics. Irrig. Sci. 27, 319–330.

Geerts, S., Raes, D., Garcia, M., Condori, O., Mamani, J., Miranda, R., Cusicanqui, J., Taboada, C., Yucra, E., Vacher, J., 2008. Could deficit irrigation be a sustainable practice for quinoa (*Chenopodium quinoa* Willd.) in the Southern Bolivian Altiplano? Agric. Water Manag. 95, 909–917.

Gowing, J.W., Rose, D.A., Ghamarnia, H., 2009. The effect of salinity on water productivity of wheat under deficit irrigation above shallow groundwater. Agric. Water Manag. 96, 517–524.

Hie, Q., Cui, B.S., Zhao, X.S., Fu, H.L., 2008. Niches of plant species in wetlands of the Yellow River Delta under gradients of water table depth and soil salinity. Chin. J. Appl. Ecol. 19, 969–975 (in Chinese).

Homaee, M., Dirksen, C., Feddes, R.A., 2002a. Simulation of root water uptake I. Non-uniform transient salinity using different macroscopic reduction functions. Agric. Water Manag. 57, 89–109.

Homaee, M., Feddes, R.A., Dirksen, C., 2002b. A macroscopic water extraction model for nonuniform transient salinity and water stress. Soil Sci. Soc. Am. J. 66, 1764–1772.

Il'Ichev, A.T., Tsypkin, G.G., Pritchard, D., Richardson, C.N., 2008. Instability of the salinity profile during the evaporation of saline groundwater. J. Fluid Mech. 614, 87–104.

Kahlown, M.A., Ashraf, M., Zia ul, H., 2005. Effect of shallow groundwater table on crop water requirements and crop yields. Agric. Water Manag. 76, 24–35.

Li, G.X., Wei, H.L., Han, Y.S., Chen, Y.L., 1998. Sedimentation in the Yellow River delta, part I: flow and suspended sediment structure in the upper distributary and the estuary. Mar. Geol. 149, 93–111.

Liu, C.M., Zhang, S.F., 2002. Drying up of the Yellow River: its impacts and countermeasures. Mitig. Adapt. Strategies Glob. Chang. 7, 203–214.

Morris, J.D., Collopy, J.J., 1999. Water use and salt accumulation by *Eucalyptus camaldulensis* and *Casuarina cunninghamiana* on a site with shallow saline groundwater. Agric. Water Manag. 39, 205–227.

Mualem, Y., 1976. A new model for predicting the hydraulic conductivity of unsaturated porous media. Water Resour. Res. 12, 513–522.

Richards, L.A., 1954. Diagnosis and Improvement of Saline and Alkali Soils United States Salinity Laboratory Staff, Agricultural Handbook No. 60. United States Department of Agriculture, Washington, DC, USA.

Šimůnek, J., van Genuchten, M.Th., Šejna, M., 2005. The HYDRUS-1D Software Package for Simulating the Movement of Water, Heat, and Multiple Solutes in Variably Saturated Media, Version 3.0. HYDRUS Software Series 1. Department of Environmental Sciences, University of California Riverside, Riverside, California, USA, 270 pp.

Šimůnek, J., van Genuchten, M.Th., Šejna, M., 2008. Development and applications of the HYDRUS and STANMOD software packages and related codes. Vadose Zone J. 7, 587–600.

Singh, R., van Dam, J.C., Feddes, R.A., 2006. Water productivity analysis of irrigated crops in Sirsa district, India. Agric. Water Manag. 82, 253–278.

Song, C.Y., Liu, G.Y., Liu, Q.S., Cao, M.C., Huang, C., 2008. Distribution patterns of plant communities in the Yellow River Delta and related affecting factors. Chin. J. Ecol. 27, 2042–2048 (in Chinese).

Tan, X., Zhao, X., 2006. Spatial distribution and ecological adaptability of wetland vegetation in Yellow River Delta along a water table depth gradient. Chin. J. Ecol. 25, 1460–1464 (in Chinese).

van Genuchten, M.Th., 1987. A numerical model for water and solute movement in and below the root zone. Research Report No. 121. U.S. Salinity Lab., Riverside, CA, USA.

van Genuchten, M.T., 1980. A closed-form equation for pre-dicting the hydraulic conductivity of unsaturated soils. Soil. Sci. Soc. Am. J. 40, 892–898.

Vazifedoust, M., van Dam, J.C., Feddes, R.A., Feizi, M., 2008. Increasing water productivity of irrigated crops under limited water supply at field scale. Agric. Water Manag. 95, 89–102.

Wang, F.Y., Liu, R.J., Lin, X.G., Zhou, J.M., 2004a. Arbuscular mycorrhizal status of wild plants in saline-alkaline soils of the Yellow River Delta. Mycorrhiza 14, 133–137.

Wang, X.G., Hollanders, P.H.J., Wang, S.L., Fang, S.X., 2004b. Effect of field groundwater table control on water and salinity balance and crop yield in the Qingtongxia Irrigation District, China. Irrig. Drain. 53, 263–275.

Wang, Y.G., Xiao, D.N., Li, Y., Li, X.Y., 2008. Soil salinity evolution and its relationship with dynamics of groundwater in the oasis of inland river basins: case study from the Fubei region of Xinjiang Province, China. Environ. Monit. Asses. 140, 291–302.

Xiong, X., He, Q., Cui, B.S., 2008. Double principal coorclinate analysis of herbaceous vegetation in wetlands of the Yellow River Delta, China. Chin. J. Ecol. 27, 1631–1638 (in Chinese).

Yang, J.F., Wan, S.Q., Deng, W., Zhang, G.X., 2007. Water fluxes at a fluctuating water table and groundwater contributions to wheat water use in the lower Yellow River flood plain, China. Hydrol. Proc. 21, 717–724.

Zacharias, I., Dimitriou, E., Koussouris, T., 2005. Integrated water management scenarios for wetland protection: application in Trichonis Lake. Environ. Model. Softw. 20, 177–185.

Zhang, G.S., Wang, R.Q., Song, B.M., 2007. Plant community succession in modern Yellow River Delta, China. J. Zhejiang Univ. Sci. B 8, 540–548.

Zong, X.Y., Liu, G.H., Qiao, Y.H., Cao, M.C., Huang, C., 2008. Dynamic changes of wetland landscape pattern in the Yellow River delta based on GIS and RS. In: Li, G., Jia, Z., Fu, Z. (Eds.), 2008 Proceedings of Information Technology and Environmental System Sciences. Publishing House of Electronics Industry, Beijing, pp. 1114–1118.

Zuo, Q., Meng, L., Zhang, R.D., 2004. Simulating soil water flow with root-water-uptake applying an inverse method. Soil Sci. 169, 13–24.